Imaging the Dimers in Si(111)-(7 × 7)

E. Bengu, R. Plass, and L. D. Marks
Department of Materials Science and Engineering, Northwestern University, Evanston, Illinois 60208

T. Ichihashi, P. M. Ajayan,* and S. Iijima
NEC Corporation, Fundamental Research Labs, Tsukuba, Ibariki 305, Japan

(Received 8 July 1996)

High resolution electron microscope images of the Si(111)-(7 × 7) surface in the plan-view geometry have been analyzed, and the overlap of the top and bottom surfaces has been extracted numerically. The resultant images show clearly not just the adatoms seen by scanning tunneling microscopy but all the atoms in the top three layers, including the dimers in the third layer. [S0031-9007(96)01560-8]

PACS numbers: 68.35.Bs, 61.16.Bg, 79.60.Bm

The Si(111)-(7 × 7) surface is one of the most, if not the most, complicated surface structure in existence. A mystery for many years, the first reasonably accurate structure model came from transmission electron diffraction data (TED) [1,2], assisted in part by the observation of adatoms by scanning tunneling microscopy (STM) [3–6]. The results of grazing incidence x-ray diffraction [7–9], low energy electron diffraction (LEED) [10,11], TED [1,2,12], as well as theoretical analyses [13–17], are in agreement with the so-called dimer-adatom-stacking (DAS) model. This model consists of 12 adatoms (first layer), a stacking fault bilayer (second and third layer) within which 9 dimers (third layer) border the triangular subunits as the core structure of $\frac{1}{6}[112]$ screw dislocations, and a deep vacancy at each apex of the unit cell.

While STM was used successfully to image the adatoms on the surface, many of the key features, for instance, the dimers in the third layer, are too deep in the structure. Another technique, high resolution electron microscopy (HREM), can obtain atomic scale information about surfaces by direct imaging. First employed in the so-called profile imaging mode [18], there has been slow progress over the past few years using the more general plan-view mode [19], where the electron beam is perpendicular to the surface of interest. In particular, the use of noise reduction filters [20] has enabled images to be obtained at very high resolutions in one case [21].

In this Letter we report results obtained using plan-view imaging coupled with noise reduction and numerical inversion to separate the top and bottom surfaces. The resultant images clearly show not just the adatoms but also the buried dimers.

The sample was prepared from a *p*-type Si(111) wafer of 10–20 Ohm cm. A disk of 3 mm diameter was cut from the wafer, then mechanically thinned and dimpled. Chemical etching of the specimen was performed using a HF + HNO_3 solution. In this fashion the specimen develops pits on its surface, and thin regions in the pits are less than 300 Å thick. The specimen surface was cleaned by heating at 1300 °C, using an infrared light in an ultrahigh vacuum chamber linked to a newly developed ultrahigh vacuum transmission electron microscope (JEM-2000FXV, operated at 200 kV, resolution 2 Å). The vacuum around the specimen during cleaning was in the 10^{-8} Torr range, and during observation it was kept in the 10^{-10} Torr range.

The experimental images were obtained with a zone axis orientation, in which case one should use a full dynamical model with nonlinear imaging for the bulk reflections. However, here we are interested only in the weak (2%–3%) surface reflections, for which a kinematical approximation with linear imaging will be rather accurate. (The highly nonlinear bulk {220} beams were digitally removed before separation of the images took place.) Neglecting any focal difference between the top and bottom surface, in this approximation the electron wave leaving the sample can be written as

$$\Psi(\mathbf{r}) = 1 + i\sigma[V(\mathbf{r}) + V(\mathbf{d} - \mathbf{r})], \tag{1}$$

giving an image $I(\mathbf{r})$,

$$I(\mathbf{r}) = 1 + \int \sigma T(\mathbf{u})\{V(\mathbf{u}) + V^*(\mathbf{u})\exp(2\pi i\mathbf{d}\cdot\mathbf{u}\} \times \exp(-2\pi i\mathbf{u}\cdot\mathbf{r})d\mathbf{u} + \eta(\mathbf{r}), \tag{2}$$

where $V(\mathbf{r})$ is the potential of the top surface, σ the relativistic interaction constant, $T(\mathbf{u})$ includes the microscope aberrations, $\mathbf{d}$ the translation between the top and bottom surfaces, and $\eta(\mathbf{r})$ the noise in the images. This translation can take any of the 49 possible combinations of 1 × 1 lattice translations within the unit cell, plus one of the three translations (0, 0), $(\frac{1}{3}, \frac{2}{3})$, and $(\frac{2}{3}, \frac{1}{3})$ due to the three different terminations *A*, *B*, or *C* of the *ABCABC* bilayer stacking. Hence, there are a total of 147 possible translations. Assuming *p*6*mm* symmetry, there is sufficient information, in principle, to determine the translation directly numerically as a free variable. However, in

 0031-9007/96/77(20)/4226(3)$10.00 © 1996 The American Physical Society

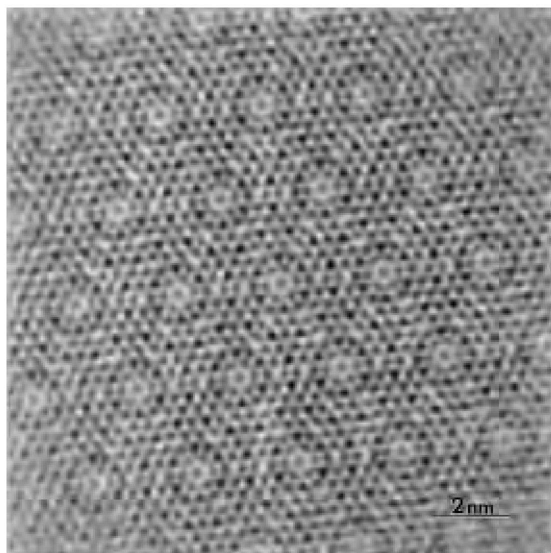

FIG. 1. A separated part of the image 1 from a 1024 × 1024 pixel region after rotational (threefold) averaging. Atoms are black, with slightly darker features at the adatom locations where two atoms are superimposed.

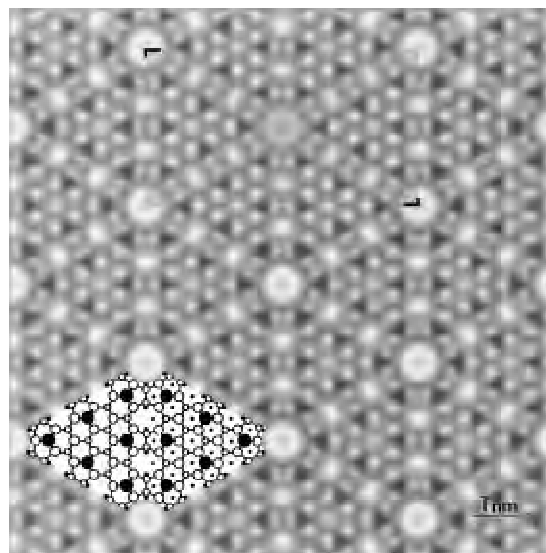

FIG. 2. A separated, rotationally (sixfold) and translationally averaged image from image 1. The inset is an image simulation for a defocus of −36 nm. Atoms are black, with slightly darker features at the adatom locations where two atoms are superimposed.

practice, a less noise sensitive methodology was used for finding which of the possible translations generated the best $R(\mathbf{u}) = T(\mathbf{u})V(\mathbf{u})$, best in the sense of least squares error between symmetry equivalent Fourier coefficients. [Here $R(\mathbf{r})$, the inverse Fourier transform of $R(\mathbf{u})$, is the image of a single surface.]

To be specific, in Fourier space we used the Wiener filter

$$R(\mathbf{u}) = I(\mathbf{u})A^*(\mathbf{u})/[|A(\mathbf{u})|^2 + |\eta(\mathbf{u})|^2], \quad (3)$$

with

$$A(\mathbf{u}) = 1 + \exp(2\pi i\mathbf{u} \cdot \mathbf{d}) \quad (4)$$

estimating the noise from radial sections and then either removing the noise first [20] [and using a small positive value for $\eta(\mathbf{u})$ in Eq. (3) as a pseudoinverse] or including this estimate directly; the results were independent of the method used.

Using this strategy, we than determined $R(\mathbf{r})$ for two different images (image 1 and image 2 with different defocus) using large areas (1024 × 1024 pixels). For image 1, separation of the bottom and top surfaces was done for three different regions, and, for image 2, only one region was used.

Part of a large area, separated and subsequently (threefold) rotationally averaged from image 1, is shown in Fig. 1. Evident are all the main details of the structure with "black atoms," not just the adatoms but also the dimers. This is even more apparent for the rotationally and translationally averaged image in Fig. 2. The inset in Fig. 2 is a multislice image simulation for a defocus of −36 nm performed using a 3-layer model which matches exceedingly well.

As a cross-check, Fig. 3 shows the results from image 2 separation and translational averaging, with an image simulation inset. While at this particular defocus (−136 nm) one cannot directly see the atomic structure, the correspondence between the experimental and calculated images is fairly good. In fact, there are differences between the images; the calculated image has the opposite phase compared to the experimental one, in particular, for three reflections [(5, 0), (7, 2), and (4, 4)]. If we obtained

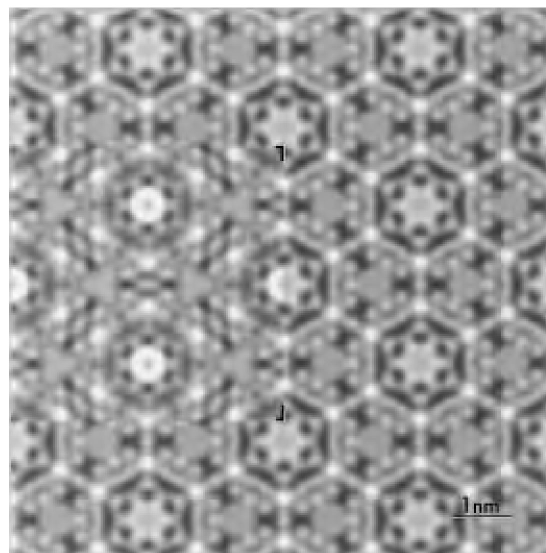

FIG. 3. A rotationally (sixfold) and translationally averaged image after separation which fits at a defocus of −136 nm, as shown by the image simulation inserted.

such a match for a bulk crystal using conventional HREM, we would not be satisfied; however, considering the low signal levels, the neglect of dynamical diffraction and subsurface strains, as well as image astigmatism and tilt, the agreement is reasonable.

The experimental data herein clearly show all the primary features of the DAS model, the dimers as well as the adatoms. This illustrates the difference between HREM as an imaging technique and STM; HREM not only shows the outermost surface but also the layers underneath. It is a point of some relevance that the images that we employed herein are by no means testing the intrinsic resolution of the microscope; in fact, we are only using information out to about 2.5 Å. The major factor limiting the available resolution is noise, which originates almost exclusively from relatively poor counting statistics and low contrast levels (2%–3%). Of the two, shot noise is the primary limitation. This is not, in fact, an intrinsic problem, and, by using longer exposures and higher beam fluxes (for instance, field emission sources), it should be realistic to reduce the noise by perhaps a factor of 5–10. At this level, direct information about dimer configurations at, for example, domain boundaries and other types of defects should become directly accessible.

Two small points merit clarification; first, our use of $p6mm$ symmetry here. From LEED [11], theoretical studies [13–17], and STM [22], there is evidence for a small deviation to $p3m1$ symmetry. As noted by Twesten and Gibson [12], this is small and has relatively minor effects upon the low-order beam intensities. There will be a small phase change, which, from electron diffraction data [23], we can estimate to be about 5 degrees, far less than the errors in the experimentally measured amplitudes. In the future, with better data, it may be possible to improve on our method and use lower symmetries. The second point concerns our neglect of focus differences between the top and bottom surfaces. This will lead to a small effect, even if we make the pessimistic estimate that the crystal is as thick as 10 nm, when working around the Scherzer defocus or another pass band. In thicker crystals, this type of effect [24] needs to be considered.

This work was supported by NSF Grant No. DMR-9214505 (E. B. and L. D. M.), AFOSR Grant No. F49620-92-J-0250 (R. P.), and partial support from the NEDO Grant (T. I., P. M. A., and S. I.).

*Current address: Max-Planck-Institut für Metallforschung, Institut für Werkstoffwissenschaft, Seestrasse 92, 70174 Stuttgart, Germany.

[1] K. Takayanagi, Y. Tanishiro, M. Takahashi, and S. Takahashi, J. Vac. Sci. Technol. A **3**, 1502 (1985).
[2] K. Takayanagi, Y. Tanishiro, S. Takahashi, and M. Takahashi, Surf. Sci. **164**, 367 (1985).
[3] G. Binnig, H. Rohrer, Ch. Gerber, and E. Weibel, Phys. Rev. Lett. **50**, 120 (1983).
[4] H. Tanaka, M. Udagawa, M. Itoh, T. Uchiyama, Y. Watanabe, T. Yokotsuka, and I. Sumita, Ultramicroscopy **42–44**, 864 (1992).
[5] H. Tokumoto and M. Iwatsuki, Jpn. J. Appl. Phys. **32**, 1368 (1993).
[6] Y.-N. Yang and E. D. Williams, Scanning Microsc. **8**, 781 (1994).
[7] I. K. Robinson, W. K. Waskiewicz, P. H. Fuoss, J. B. Stark, and P. A. Bennett, Phys. Rev. B **33**, 7013 (1986).
[8] I. K. Robinson, W. K. Waskiewicz, P. H. Fuoss, and L. J. Norton, Phys. Rev. B **37**, 4325 (1988).
[9] J. Skov Pedersen, R. Feidenhans'l, M. Nielsen, F. Grey, and R. L. Johnson, Phys. Rev. B **38**, 13 210 (1988).
[10] R. E. Schlier and H. E. Farnsworth, J. Chem. Phys. **30**, 917 (1959).
[11] H. Huang, S. Y. Tong, W. E. Packard, and M. B. Webb, Phys. Lett. A **130**, 166 (1988).
[12] R. D. Twesten and J. M. Gibson, Ultramicroscopy **53**, 223 (1994).
[13] K. Takayanagi, Y. Tanishiro, and K. Kajiyama, J. Vac. Sci. Technol. B **4**, 1074 (1986).
[14] Guo-Xin Qian and D. J. Chadi, J. Vac. Sci. Technol. B **4**, 1079 (1986).
[15] P. Badziag and W. S. Verwoerd, Phys. Rev. B **40**, 1023 (1989).
[16] Guo-Xin Qian and D. J. Chadi, Phys. Rev. B **35**, 1288 (1987).
[17] J. P. LaFemina, Surf. Sci. Rep. **16**, 133 (1992).
[18] L. D. Marks, Phys. Rev. Lett. **51**, 1000 (1983); L. D. Marks and D. J. Smith, Nature (London) **303**, 316 (1983).
[19] G. Jarayam, R. Plass, and L. D. Marks, Interface Sci. **2**, 381 (1995).
[20] L. D. Marks, Ultramicroscopy **62**, 43 (1996).
[21] R. Plass and L. D. Marks, Phys. Rev. Lett. **75**, 2172 (1995).
[22] J. Nogami (private communication).
[23] Electron diffraction intensities taken from Ref. [12] were supplied by Dr. R. Twesten; a description of the results of this analysis is in preparation.
[24] L. D. Marks and R. Plass (unpublished).